Ber. Ohara Inst. landw. Biol., Okayama Univ. 18 : 183–209 (1984)

GOUDRIAAN'S MODEL OF CROP MICROMETEOROLOGY APPLIED TO THE RICE CROP+

Yoshio HIRAMATSU*, Takuro SEO
and Toshihiko MAITANI

INTRODUCTION

Interactions between a crop and its surroundings constitute a micrometeorology characteristic of the crop. In principle, crop micrometeorology can be described by a set of transport equations involving source terms. In practice, the interactions are complex, and the analyais of crop micrometeorology has necessarily recourse to modelling. A number of models simulating crop micrometeorology have been proposed (Waggoner 1975). The model of Goudriaan (1977) is the most comprehensive and relatively free from a priori assumptions.

Goudriaan described in detail his model in a monograph published in 1977. This model simulates the crop micrometeorology with given daily runs of meteorological parameters at a height above the crop; relevant properties of the crop and the soil need to be prescribed.

The Wageningen group tested the model using the data obtained during the daytime in a maize field (Goudriaan 1977; Stigter et al. 1977). The model remains to be tested for different types of crop and in various climates. This paper presents the model results compared with measurements for a rice field.

MICROMETEOROLOGICAL OBSERVATION IN A RICE FIELD

1. *Observation Conditions*

The observation was planned to provide the input data in the simulation and the data to be compared with model results.

The observation was made in a rice field (300 m × 300 m) of the University Farm located at Hachihama (34.5°N, 136°E) on September 17/18, 1980. It was started at 2h20m on September 17 and continued for 24 hours.

The crop was at the early stage of ripening and the average crop height was 75 cm. The number of plants was 25 to 30 per square meter with a leaf area index of 3.6. The field was not flooded, but the soil

Received November 7, 1983.
+ This research was partly supported by the Ministry of Education, Science and Culture under the Grant-in-Aid for Scientific Research No. 56480045.
* Present affiliation: Mabi Higashi Secondary School, Mabi-cho, Okayama Pref.

was almost saturated with water.

The weather was generally fair with a hazy sky. Daytime winds were light to moderate, and prevailingly northeast in the morning and southeast in the afternoon. Winds at night were calm to light, and variable in the direction. Stability conditions are shown in Fig. 7.

2. *Instrumentation*

Net radiation was measured at 80 cm above the canopy with a Funk-type net radiometer (EIKO CN-1). The output signal was recorded on a potentiometric pen recorder.

Air temperature and wet-bulb temperature were measured at five heights above the ground (190, 107, 75, 45, 22 cm) with thermocouple psychrometers equipped with radiation shields. Temperature directly below the soil surface and soil temperature at 5 cm depth were measured with thermocouple thermometers. The thermocouple signals were recorded on a 12-point potentiometric recorder of 1.5 mV range; the recorder scans the signals sequentially at 5 sec intervals.

Horizontal components of wind u (streamwise) and v (traverse) were measured at a height 156 cm with a 2-dimensional sonic anemometer (KAIJODENKI PAS 211-1). Vertical wind component w was measured with a 1-dimensional sonic anemometer (KAIJODENKI PA 112). Fluctuations of air temperature and water vapor pressure were measured

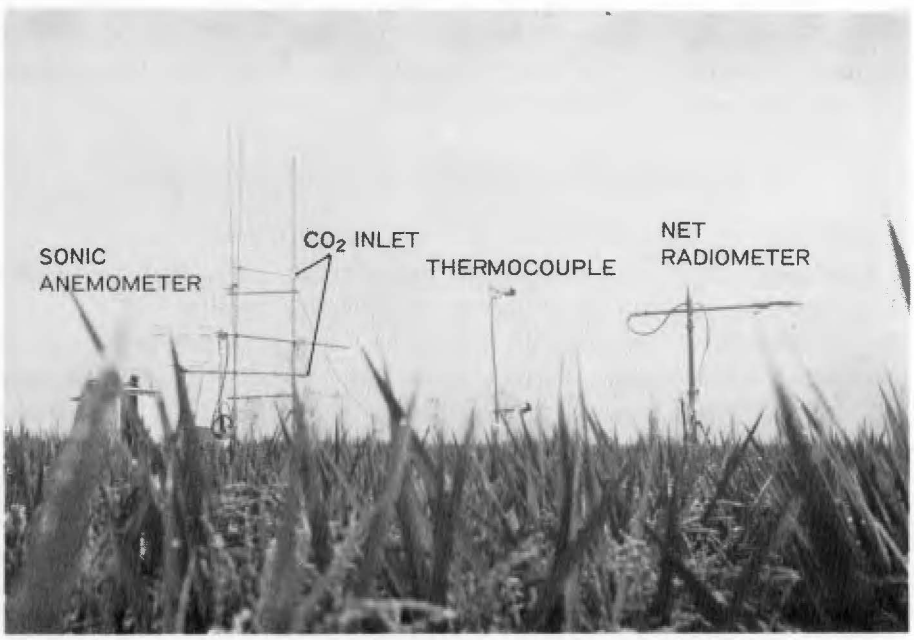

FIG. 1. Installation of the instruments (September 17, 1980 Hachihama). View toward northeast.

with a fine-wire thermocouple psychrometer. The outputs of these fast response instruments were recorded on an analog tape recorder. The psychrometer sensor and w-sensor were deployed to give turbulent fluxes of heat and vapor at a height of 156 cm. The instrumentation for measuring turbulent fluxes was the same as described in Takeuchi et al. (1980).

Difference in CO_2 concentration was measured between 212 cm and 102 cm above the ground with an infrared gas analyser (URAS 2) with a 50 ppm range operated in differential mode. Air was sampled at intakes located at the two heights specified above and conducted through vinyl tubings to the analyser. For full description of the measuring system, see Ohtaki and Seo (1972). CO_2 concentration was occasionally (at about 3 hr intervals) measured with the same analyser. For this purpose the difference measurement was temporally interrupted and CO_2 gas of known concentration was passed through the reference cell.

The instruments were installed as depicted in Fig. 1. Signal conditioners, recorders and the gas analyser were housed in an observation hut located about 20 m northwest of the measuring site.

3. *Data Processing*

The data were processed for each consecutive period of 10 min; thus, the averaging time of the statistics (mean value and covariance) is 10 min.

The signals from the sonic anemometers and fine-wire thermocouple psychrometer were processed using the data processing system described in Maitani and Seo (1976). The data stored in analog tapes were reproduced, and digitized at intervals of 0.08 sec. Fluxes of momentum, heat and water vapor were evaluated by the eddy correlation method. Vapor pressure was calculated from psychrometer data using Sprung's formula.

The CO_2 flux above the canopy was estimated as follows. The water vapor flux $\overline{w'q'}$ and the difference of specific humidity Δq between two heights z_1 and z_2 are given by the measurement. w' and q' are fluctuations of vertical wind and specific humidity respectively, and the bar denotes a time averaging. The eddy diffusivity K_q at a height of $z_q - d = \sqrt{(z_1-d)(z_2-d)}$ is estimated as

$$K_q = -\overline{w'q'}/(\Delta q/\Delta z)$$

with $\Delta z = z_1 - z_2$, $z_1 = 1.90$ m, $z_2 = 0.75$ m, and the zero-plane displacement $d = 0.45$ m. The CO_2 difference ΔC is measured between $z_1' = 2.12$ m and $z_2' = 1.02$ m. The CO_2 flux F_c in kg m^{-2} s^{-1} is calculated from ΔC in ppm by the formula

$$F_c = -\rho(M_c/M_d)K_c(\Delta C/\Delta z) \times 10^{-6}$$

where $\Delta z = z_1' - z_2'$, and $K_c = ((z_c-d)/(z_q-d))K_q$ with $z_c-d = \sqrt{(z_1'-d)(z_2'-d)}$; ρ is air density (kg m^{-3}), and $M_c = 44$ and $M_d = 29$ are molecular weight of CO_2 and dry air, respectively.

PROGRAM EXECUTION

1. *Preliminary Remarks*

Goudriaan's program as given in his monograph (1977) was used in the computation. Our computational work was started in 1979 on the NEAC ACOS6 SYSTEM 700. At that time the system could not implement CSMP used in the original program, and the program was rewritten in FORTRAN.

Two modifications of the program were taken; these do not affect the structure of the program.

1) CO_2 concentration and flux were computed by the same procedure as used in computing air temperature and humidity and their respective fluxes, i. e., by numerical integration of the transfer equations with given boundary conditions. The original program assumes a balance between flux divergence and source strength for the CO_2 transfer.

2) Test calculation by the original program yielded unprobable results for the night, in particular, very high CO_2 concentration. It was inferred that the stability correction on the eddy diffusivity was overestimated. The pertinent stability correction function

$$\phi_h = 0.74 + 4.7\zeta \text{ for } Ri \leq 0.21\,; \quad \phi_h = 1E10 \text{ for } Ri > 0.21$$

was thus replaced by

$$\phi_h = 0.74 + 4.7\zeta \text{ for } Ri \leq 0.15\,; \quad \phi_h = 5 \text{ for } Ri > 0.15$$

where ζ is the Monin-Obukhov stability parameter, and Ri is the Richardson number.

The modified function approximates Hicks' results for momentum transfer within $\zeta < 10$ (refer to the review by Carson and Richards (1978)). The effect of this modification is demonstrated in the sensitivity analysis (item 1) below.

2. *Parameters*

The parameters to be specified are listed below. Numerical values are given or their sources are indicated. Values differing from those in Goudriaan's program are placed within parenthesis. Original values are bracketed.

A1. Latitude of experimental plot (34.5°); difference in hours from standard time (0.0); number of the days in the year reckoned from 1 January (261); hours of the day when simulation is started (2.33333)
A2. Fraction of diffuse radiation as function of sun height [Goudriaan 1977, Table 1]
B1. Reference height (1.56 m)
B2. Number of layers inside canopy [3]; thickness of topmost soil layer [0.002 m]; multiplication factor for thickness of subsequent soil layers [1.2]
C1. Crop height (0.75 m); zero-plane displacement (0.45 m); roughness length (0.075 m)
C2. Leaf area index (3.6); leaf area distribution [parabolic]; leaf angle distribution [spherical]; average width of leaves (0.01 m)
C3. Scattering coefficient of leaves, for visible, nearinfrared, and longwave radiation [0.2, 0.85, 0, respectively]
C4. Drag coefficient of leaves [0.3]; intensity of turbulence within canopy [1.0]
C5. Photosynthesis-light response curve (data for rice by Horie 1980); light saturated net CO_2 assimilation as dependent on temperature (data for rice by Horie 1980); derivative of CO_2 assimilation vs. absorbed visible radiation at low light intensity (0.41 $kgCO_2\ ha^{-1}\ h^{-1}/(J\ m^{-2}\ s^{-1})$); dark respiration [$0.17 \times 10^{-6}$ $kgCO_2\ s^{-1}/m^2$ leaf area at 30°C, approx. 6 kg $ha^{-1}\ h^{-1}$]
C6. Internal CO_2 concentration maintained by stomatal regulation (210 ppm); minimal stomatal resistance as function of relative water content [Goudriaan 1977, Fig. 17]; xylem resistance to transpiration stream of water [10^7 bar m^2 s kg^{-1}]; cuticular resistance to transpiration [2000 s m^{-1}]
C7. Minimal conductance of root system [3.5×10^{-2} kgH_2O $bar^{-1}\ m^{-2}\ s^{-1}$]; reduction factor for root conductance as function of soil temperature [Goudriaan 1977, Fig. 18]; plant water stress as function of relative water content [Goudriaan 1977, Fig. 17]
D8. Soil respiration [1 g $m^{-2}\ h^{-1}$]; soil heat conductivity (0.882 J $m^{-1}\ s^{-1}\ K^{-1}$); volume heat capacity of soil (2.73×10^6 J $m^{-3}\ K^{-1}$)*; average height of clods [0.001 m]; soil surface resistance to evaporation [0 s m^{-1}]; water stress of soil [−0.1 bar]

3. *Boundary and Initial Conditions*

Fig. 2 shows the input data as boundary conditions to the model. The reference level was taken at 1.56 m, where the horizontal wind

* For soil thermal properties of paddy fields, reference is made to Seo and Yamaguchi (1968) and Seo (1958).

was measured. Values of air temperature and vapor pressure were linearly interpolated from the measurements at 1.90 m and 1.07 m. Data on net radiation, wind, air temperature, and vapor pressure were smoothed by taking 3-term moving averages. These data were stored in disk files to be retrieved during the program execution.

CO_2 concentration at the reference level was interpolated from measurements at heights of 2.12 m and 1.02 m.

Initial conditions were assigned as follows. Difference of air temperature between inside the canopy and the reference level $= -4°C$; soil temperature $= 20°C$; difference of water vapor pressure between inside canopy and the reference level $= -2$ mb; amount of dew in the canopy layer (in latent heat) $= 0$ J m^{-2}; duration of leaf wetness $= 0$ s; water content of the canopy $= 8.775 \times 10^{-3}$ kgH_2O m^{-2}.

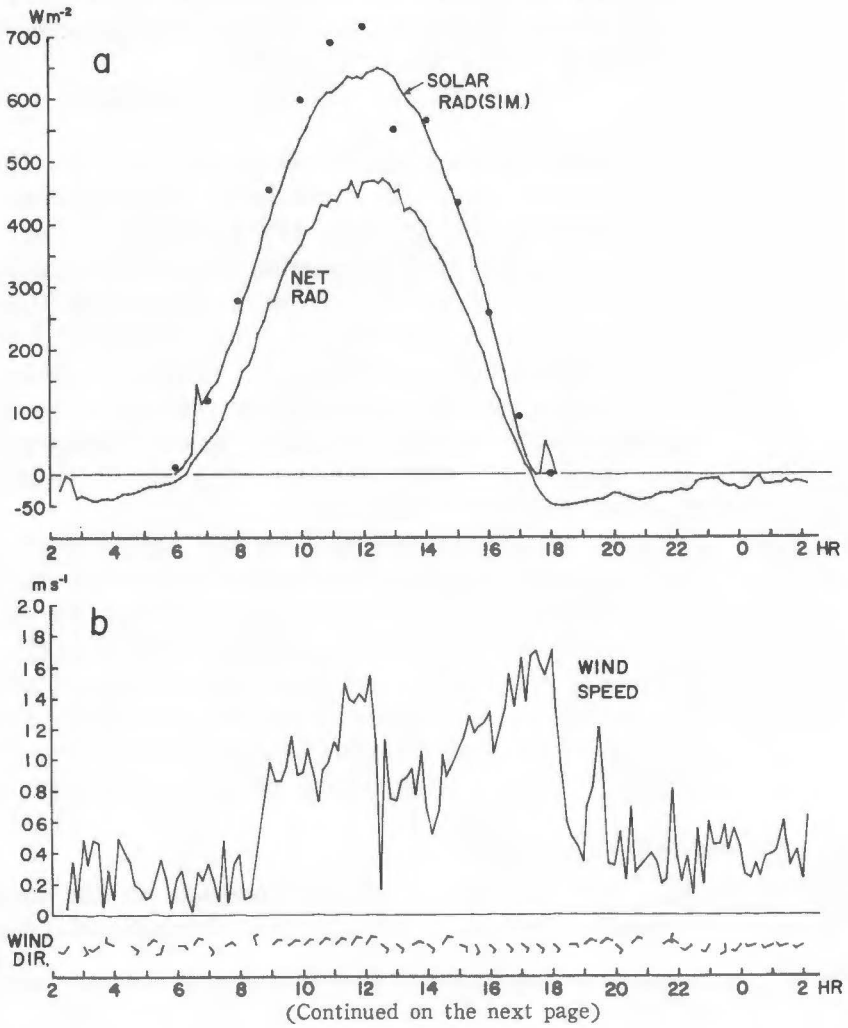

(Continued on the next page)

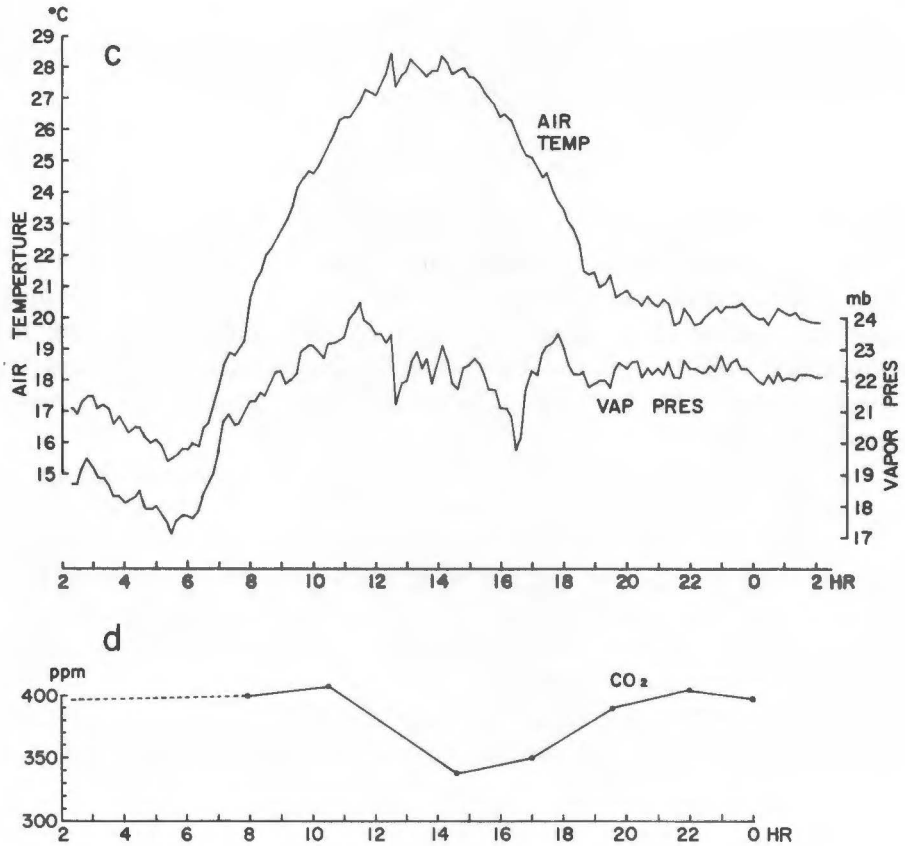

FIG. 2. Input data.

(a) Net radiation. Simulated solar radiation (—) and solar radiation measured at Kurashiki (•) are included.
(b) Wind at the reference height 1.56 m.
(c) Air temperature and water vapor pressure at the reference height 1.56 m.
(d) CO_2 concentration at the reference height 1.56 m.

4. *Outputs*

The ultimate end of the computation is prediction of diurnal variations of air temperature, water vapor pressure and CO_2 concentration in three sublayers (75–46 cm, 46–29 cm, 29–0 cm) of the canopy layer, and diurnal variations of soil temperature at the surface and in 10 substrata down to 52 cm. The computed results of these variables and the turbulent fluxes at the top and bottom of the crop layer were stored in disk files at 10 min intervals.

The results of the computation, including those for other intermediate variables, were printed on a line printer for every hour of the day. Important intermediate variables are : wind, eddy diffusivity, aerial

fluxes of heat, water vapor and CO_2 within the canopy layer; heat and mass exchange between the canopy and the surroundings, e. g., transpiration, net CO_2 assimilation and dew.

PERFORMANCE OF THE MODEL

1. *Impact of Initial Conditions and Approximation to Steady State*

Test calculation with the same input repeated for 3 successive days showed that the initial conditions have an apparent effect on the model results only immediately after the start of the computation and that the computed results for the third day insignificantly from those for the second day. Here, 'day' means the 24 hr computational period beginning at 2h20m.

The program counts the TELLFO number of times that the rate of fast processes (temporal change term of transfer equation) are set at zero. TELLFO indicated that the equilibrium between flux divergence and source strength is not usually attained during the night. Addition of CO_2 budget into the equilibrium criterion has practically no effect to improve the situation; this is confirmed in the sensitivity analysis (iteme 14) to be expounded below.

Fig. 3 shows the simulated profiles of temperature at 3 h for successive 4 days. It is noted that the initial condition at 2h20m was given

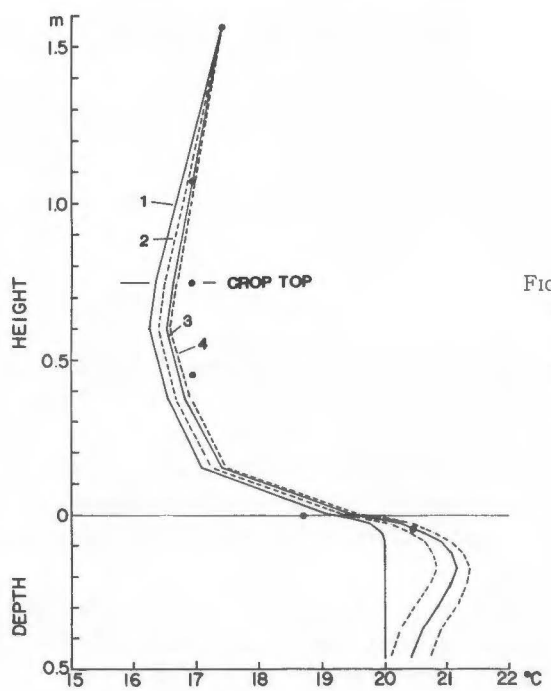

FIG. 3. Simulated temperature profiles at 3h for four successive days; measured temperatures are shown by filled circles.

as follows: above canopy temperature 17°C, air temperature in the canopy 13°C, and soil temperature 20°C. The figure shows that at 3 h of the first day the impact of the initial condition practically disappears for air temperature, but it still remains for the soil temperature below a 5 cm depth. An exact steady state is not reached even after 3 days, though the change from day to day decreases. For daytime the approximation to the steady state is better.

Henceforth, we use the outputs for the second day, unless otherwise stated.

2. *Sensitivity Analysis*

Some input variables, notable CO_2 content, could not be measured accurately enough. Parameter values and functional relationships adopted here are estimates based on previous measurements or *in situ* measurements of a small size of samples. Some of them are not well established, and others may not be representative. The effect of such uncertainties on the model output is examined by varying the values of inputs and parameters. It is noted that meteorological variables at the reference height used as inputs are not strictly external to the model in that they are influenced by the physical and plant-physiological processes underneath.

Variations taken here are as follows:

1) The functional relationship $\phi_h = 0.74 + 4.7\zeta$ is taken to apply for $Ri \leq 0.21$; for $Ri > 0.21$ $\phi_h = 1.E10$. By this change the original program is retrieved in respect of ϕ_h.

2) Fraction of diffuse radiation FRDIF (about 0.15 for high sun) is increased in view of the observed hazy sky (about 0.3 for high sun).

3a, 3b) Leaf area index LAI (3.6) is varied between 2.7 and 4.2.

4) Leaf area density distribution (parabolic) is made more top-heavy in accordance with the measurements by Uchijima (1976).

5) Ratio: (zero-plane displacement)/(crop height) (0.6) is changed to 0.7.

6) Mixing length within canopy LMIX is multiplied by $(4\pi)^{1/2}$. This change is Goudriaan's later development.

7) CO_2 content at the reference level ECO2C at 10h (400 ppm) is decreased to 350 ppm. Measurements (e. g., Takasu and Kimura 1972) indicate that CO_2 concentration on the rice field falls rapidly from high night values in the morning.

8a, 8b) Internal CO_2 concentration maintained by stomatal regulation RCO2I (210 ppm) is varied between 160 and 260 ppm.

9) Soil respiration rate SRESP (10 $kgCO_2$ ha^{-1} h^{-1}) is halved. If the field is flooded by the irrigation water, soil respiration will be practically zero.

TABLE 1. Percentage deviation of the output from the reference value brought about by varying the parameters as specified by the item number in the text

(A) 12 h of the 2nd day

Output variable	Height	Reference value	Percentage deviation due to parameter variation by item														
			1	2	3a	3b	4	5	6	7	8a	8b	9	10	11	12	13	14
DTO	75cm	0.82°C	2	7	30	6	1	14	6	24	17	24	6	7	2	5	3	3
DT(1)	60	0.97°C	1	6	15	13	0	19	7	18	14	28	3	9	0	2	0	2
DT(2)	37	1.28°C	2	9	23	21	1	25	14	16	12	26	4	12	1	2	1	3
DT(3)	15	1.11°C	3	12	30	33	2	39	26	13	8	26	0	16	0	2	1	5
DVO	75	1.80 mb	0	3	14	6	0	11	4	11	9	12	1	2	1	1	1	0
DV(1)	60	2.30 mb	0	0	4	4	0	12	1	9	7	12	0	3	0	1	0	0
DV(2)	37	3.84 mb	1	2	0	0	4	14	4	6	5	8	1	3	1	2	1	1
DV(3)	15	5.91 mb	1	1	4	1	8	13	7	3	2	5	2	2	0	0	1	0
CO2(1)	60	377 ppm	0	1	0	0	0	0	0	10	0	0	1	0	0	1	0	0
CO2(2)	37	375 ppm	0	1	0	0	0	0	0	10	0	0	1	1	0	1	0	0
CO2(3)	15	378 ppm	0	1	0	1	0	0	0	10	0	0	1	1	0	1	0	0
WIND(1)	75	0.78m/s	0	0	1	0	0	18	0	1	0	1	0	0	0	0	0	0
WIND(2)	46	0.25m/s	0	0	24	13	0	18	7	0	0	0	0	0	0	0	0	0
WIND(3)	29	0.12m/s	0	0	42	19	18	18	11	0	0	0	0	0	0	0	0	0
K(1)	75	477 cm^2/s	0	0	15	7	0	18	13	0	0	0	0	0	0	0	0	0
K(2)	46	152 cm^2/s	0	0	43	19	0	18	20	1	0	1	0	0	0	0	0	0
K(3)	29	76 cm^2/s	0	1	63	26	19	18	24	0	0	0	1	0	0	1	0	0
RICHN	156–75	−0.020	1	6	26	8	1	8	6	16	13	16	6	6	3	1	1	1
SHFL(1)	75	83.4 W/m^2	1	7	17	12	0	3	6	21	17	31	2	6	1	1	0	2
SHFL(2)	46	25.8 W/m^2	2	17	24	19	2	16	22	10	5	21	5	20	2	2	1	4
SHFL(3)	29	−7.1 W/m^2	6	12	94	65	12	75	101	38	35	27	13	14	4	3	4	9
LHFL(1)	75	296 W/m^2	1	2	6	4	0	2	3	6	5	9	1	2	0	2	1	1
LHFL(2)	46	188 W/m^2	1	0	24	15	0	5	5	1	1	2	1	2	1	3	1	1
LHFL(3)	29	126 W/m^2	1	2	45	24	0	8	10	3	3	2	1	0	1	2	2	0
CO2FL(1)	75	−31.2 kg/ha/h	1	18	9	6	0	0	0	4	10	6	14	16	3	20	3	1
CO2FL(2)	46	−6.5 kg/ha/h	3	54	29	20	0	0	0	12	38	14	69	58	11	43	12	3
CO2FL(3)	29	5.7 kg/ha/h	3	26	35	18	0	0	0	7	32	2	81	39	5	33	11	4
NCO2A(1)	75–46	24.7 kg/ha/h	0	8	19	11	0	0	0	1	0	5	0	4	1	0	0	0
NCO2A(2)	46–29	12.2 kg/ha/h	0	16	1	5	0	0	0	2	0	7	0	11	3	0	0	0
NCO2A(3)	29–0	4.2 kg/ha/h	0	26	51	43	0	0	0	4	1	13	0	38	11	0	0	0
SHLL(1)	75–46	57.9 W/m^2	0	3	13	9	1	3	2	26	22	35	1	6	0	2	0	1
SHLL(2)	46–29	32.9 W/m^2	0	11	2	0	1	4	4	14	11	22	1	13	2	2	1	1
SHLL(3)	29–0	23.7 W/m^2	0	8	14	12	3	4	5	5	0	7	1	13	1	0	0	0
LHLL(1)	75–46	108.4 W/m^2	0	6	25	15	1	2	1	15	12	20	0	3	0	1	1	0
LHLL(2)	46–29	61.4 W/m^2	0	7	16	4	1	2	2	9	7	14	1	7	1	2	0	1
LHLL(3)	29–0	29.1 W/m^2	1	4	16	3	2	2	3	3	3	7	2	9	1	2	1	1
NRADS	0	132 W/m^2	0	4	33	15	0	1	0	2	2	2	0	1	0	1	0	0
SHFLB	0	31.2 W/m^2	0	4	30	24	5	20	27	13	8	12	6	6	2	1	1	3
LHFLB	0	97.5 W/m^2	0	5	54	31	1	11	13	6	5	6	1	3	1	4	2	1
G	0	65.3 W/m^2	0	2	8	4	0	7	6	0	0	0	0	1	0	7	3	0

(B) 24 h of the 2nd day

Output variable	Height	Reference value	Percentage deviation due to parameter variation by item														
			1	2	3a	3b	4	5	6	7	8a	8b	9	10	11	12	13	14
DTO	75cm	−1.24°C	86	0	5	4	0	0	1	0	0	0	1	6	1	6	3	0
DT(1)	60	−1.26°C	85	1	5	5	2	1	1	1	0	0	0	8	3	5	2	0
DT(2)	37	−1.14°C	84	1	1	1	3	5	2	1	0	0	1	9	3	6	2	0
DT(3)	15	−0.85°C	99	0	9	7	6	13	9	0	0	0	1	12	3	9	5	0
DVO	75	−0.45 mb	347	2	20	16	7	2	3	1	1	0	2	30	8	21	7	0
DV(1)	60	−0.48 mb	316	1	21	15	7	5	3	1	3	0	2	27	5	22	9	1
DV(2)	37	−0.27 mb	508	2	9	8	21	4	15	0	1	0	5	50	11	41	18	1
DV(3)	15	0.14 mb	982	8	61	6	67	35	64	4	1	0	4	97	23	87	40	0
CO2(1)	60	610 ppm	120	0	2	1	0	0	2	0	0	0	8	5	1	0	0	0
CO2(2)	37	631 ppm	114	0	3	2	1	1	1	0	0	0	9	6	1	0	0	0
CO2(3)	15	655 ppm	108	0	4	3	0	1	0	0	0	0	10	6	1	0	0	0
WIND(1)	75	0.138m/s	33	0	0	0	0	23	0	0	0	0	0	0	0	0	0	0
WIND(2)	46	0.044m/s	33	0	25	13	0	23	7	0	0	0	0	0	0	0	0	0
WIND(3)	29	0.022m/s	33	0	43	20	18	23	11	0	0	0	0	0	0	0	0	0
K(1)	75	82 cm²/s	41	0	14	7	0	25	12	0	0	0	0	0	0	0	0	0
K(2)	46	29 cm²/s	21	0	40	17	0	19	20	0	0	0	0	0	0	0	0	0
K(3)	29	19 cm²/s	6	1	39	15	5	12	22	1	0	0	1	1	0	1	0	0
RICHN	156–75	0.25	96	0	4	8	4	8	4	0	4	0	0	8	4	4	0	0
SHFL(1)	75	−2.30W/m²	100	1	5	4	1	10	1	1	0	0	0	7	3	5	2	0
SHFL(2)	46	1.91W/m²	55	3	19	13	3	9	1	3	1	1	3	5	2	8	1	2
SHFL(3)	29	2.98W/m²	30	4	2	8	0	5	2	2	1	0	2	1	1	5	6	2
LHFL(1)	75	−1.31W/m²	100	1	21	15	8	4	2	1	1	0	2	27	5	22	8	1
LHFL(2)	46	4.80W/m²	28	1	11	2	2	5	5	1	0	0	2	3	2	3	4	1
LHFL(3)	29	6.36W/m²	10	1	3	11	3	5	8	1	0	0	0	1	1	1	1	1
CO2FL(1)	75	21.4kg/ha/h	100	1	5	4	1	7	5	0	1	0	24	15	3	1	0	1
CO2FL(2)	46	17.7kg/ha/h	75	1	5	3	1	7	3	1	0	1	29	13	3	1	1	0
CO2FL(3)	29	13.9kg/ha/h	60	1	2	1	1	6	3	1	1	0	37	8	1	1	1	1
NCO2A(1)	75–46	−3.61kg/ha/h	0	0	25	17	0	0	0	0	0	0	0	33	9	0	0	0
NCO2A(2)	46–29	−3.61kg/ha/h	0	0	25	17	0	0	0	0	0	0	0	33	8	0	0	0
NCO2A(3)	29–0	−3.61kg/ha/h	0	0	25	17	0	0	0	0	0	0	0	33	6	0	0	0
SHLL(1)	75–46	−4.01W/m²	25	16	0	14	4	1	1	10	3	0	5	7	10	8	4	5
SHLL(2)	46–29	−0.99W/m²	6	31	48	10	13	14	1	16	2	0	8	15	13	11	24	9
SHLL(3)	29–0	0.25W/m²	275	46	272	279	55	291	76	29	1	1	10	73	17	15	49	11
LHLL(1)	75–46	−6.35W/m²	1	10	700	2	1	3	5	7	2	0	2	1	5	6	2	3
LHLL(2)	46–29	−1.67W/m²	45	20	31	56	10	2	19	11	1	0	7	11	4	10	11	5
LHLL(3)	29–0	0.56W/m²	277	27	1566	338	4	2	66	14	2	0	55	54	13	2	16	7
NRADS	0	−7.8W/m²	35	1	6	6	1	14	12	1	0	0	3	1	0	1	0	1
SHFLB	0	2.7W/m²	5	0	22	19	4	4	11	0	0	0	4	4	4	4	4	0
LHFLB	0	6.2W/m²	8	0	19	19	3	8	8	0	0	0	0	2	0	3	2	0
G	0	−16.7W/m²	20	0	8	5	2	4	0	0	0	0	1	2	1	2	1	0

1) Negaive values are marked by underbar.
2) Explanation of abbreviations:
DTO, DT(1), DT(2), DT(3): air temperature difference between the specified height and the reference height
DVO, DV(1), DV(2), DV(3): vapor pressure difference between the specified height and the reference height
CO2(1), CO2(2), CO2(3): CO_2 concentration
WIND(1), WIND(2), WIND(3): wind speed
K(1), K(2), K(3): eddy diffusivity for heat and vapor transfer
RICHN: Richardson number for the specified layer
SHFL(1), SHFL(2), SHFL(3): aerial flux of sensible heat
LHFL(1), LHFL(2), LHFL(3): aerial flux of latent heat
CO2FL(1), CO2FL(2), CO2FL(3): aerial flux of CO_2
NCO2A(1), NCO2A(2), NCO2A(3): net CO_2 assimilation of canopy
SHLL(1), SHLL(2), SHLL(3): release of sensible heat by canopy
LHLL(1), LHLL(2), LHLL(3): release of latent heat of transpiration by canopy
NRADS: net radiation at the soil surface
SHFLB: sensible heat flux at the soil surface
LHFLB: latent heat flux at the soil surface
G: soil heat flux
These abbreviations are the names of variables in the Goudriaan's program.

10) Dark respiration rate of leaves DPL at 30°C (6 $kgCO_2$ ha^{-1} h^{-1}) is decreased to 4 $kgCO_2$ ha^{-1} h^{-1}.

11) DPL is made dependent on the surrounding air temperature within canopy. In the original program it depends on the air temperature at the reference height.

12) Thermal conductivity of the soil LAMBDA (0.822 J m^{-1} s^{-1} K^{-1}) is increased to 1.02 J m^{-1} s^{-1} K^{-1}.

13) Volume heat capacity of the soil VHCAP (2.73×10^6 J m^{-3} K^{-1}) is increased to 2.94×10^6 J m^{-3} K^{-1}.

14) CO_2 balance of the canopy layer is added to the criterion of the equilibrium in the fast processes. In the original mode the criterion is evaluated by the heat and moisture budgets.

Abbreviations in roman capitals given above, e. g., FRDIF, ECO2C, RCO2I, are the names of parameters of variables in Goudriaan's program.

Table 1 shows the results of the sensitivity analysis for 12 h and 24 h of the 2 nd day.

RESULTS AND DISCUSSIONS

1. *Comparison between Model and Measurements*

(1) *Solar Radiation* In the present application of the model, solar radiation is calculated by the radiation submodel. Fig. 2 shows the time variation of the computed solar radiation. The figure includes solar radiation measured at Kurashiki located about 15 km northwest of

the site. The computed results appear realistic except for spikes in the morning and in the evening. As discussed by Goudriaan (1977), the model is prone to erratic behavior at low values of radiation.

The relation between calculated solar radiation and measured net radiation is nearly linear (Fig. 4). The regression gives average albedo

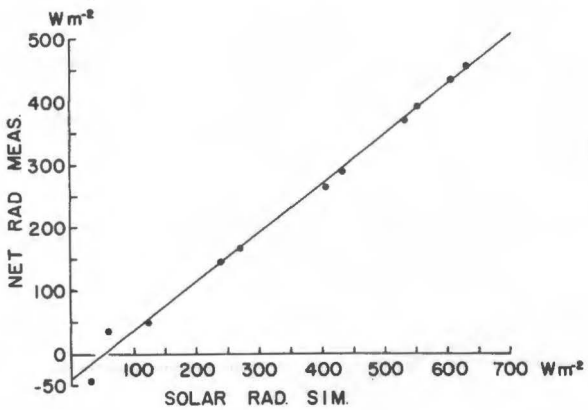

FIG. 4. Relationship between simulated solar radiation and measured net radiation.

of 20% and average daytime longwave radiation of $-50\ \mathrm{W/m^2}$. These values are reasonable; for albedo, see Seo (1972).

(2) *Momentum Flux* Momentum flux is treated in terms of shearing velocity u_*. Measured u_* represents $\sqrt{-\overline{u'w'}}$, where u' and w' are fluctuations in streamwise and vertical components of wind. The computed value results from the flux-gradient relationship

$$u_* = ku_r \Big/ \int_{d+z_0}^{z_r} \left\{\phi_m\left(\frac{z'-d}{L}\right)\Big/(z'-d)\right\} dz'$$

where u_r is the wind speed at the reference height z_r, z_0 is the rougness length, and k is the von Kármán constant. ϕ_m is the non-dimensionalized wind gradient as a function of the stability parameter $\zeta=(z-d)/L$.

Fig. 5 shows that computed results follow the variation of the measured u_*. However, at night the model consistently gives underestimates.

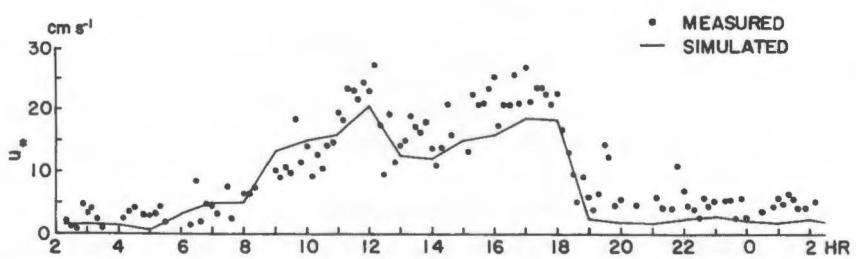

FIG. 5. Time variations of measured and simulated shearing velocity.

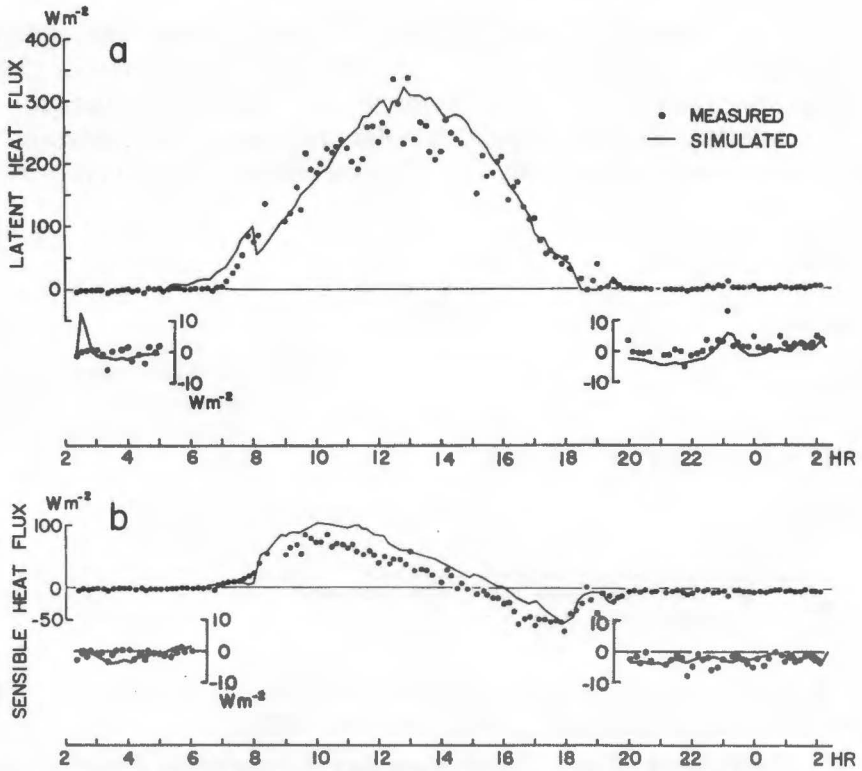

FIG. 6. Time variations of measured and simulated heat fluxes.
(a) Latent heat flux. (b) Sensible heat flux.
Night values are represented in an expanded scale.

(3) *Latent Heat Flux* Fig. 6a shows the diurnal variation of latent heat flux above the crop canopy.

The simulated latent heat flux compares well with the observation. The agreement will be made closer, if we consider that the measuring system tends to underestimate the evaporative flux. This underestimate is primarily due to the inadequate response of the wet-bulb thermocouple (Takeuchi et al. 1980). The daytime total of evapotranspiration amounts to 3 mm. This value is within the range previously obtained over a paddy field (Seo and Yamaguchi 1968).

The model reveals a remarkable variation in the morning, i. e., a rapid increase of evaporation interrupted by a transient fall; this reflects the fact that the model simulates evaporation of the dew deposited on the plant leaves at night. The corresponding feature could not be detected in the present observation.

(4) *Sensible Heat Flux* Fig. 6b shows that the variation of the computed sensible heat flux is similar to the observed diurnal variation. However, the model overestimates the daytime upward heat flux. As a

result, the time of transition from upward to downward flux in the late afternoon is later in the model than is actually observed.

In the model, the increase of upward heat flux is retarded in the morning. This is associated with the evaporation of dew mentioned above.

(5) *Stability Parameter* Comparison is made of the stability parameter $\zeta=(z-d)/L$ with $z-d=1$ m in Fig. 7. The Monin-Obukhov length L is determined from measurements as

$$L = -u^3{}_* T_v/(kg\overline{w'T_v'})$$

where T_v is the virtual temperature, T_v' is its fluctuation, and g is the acceleration of gravity. The model value of L is calculated in the scheme of evaluation of flux-gradient relationship.

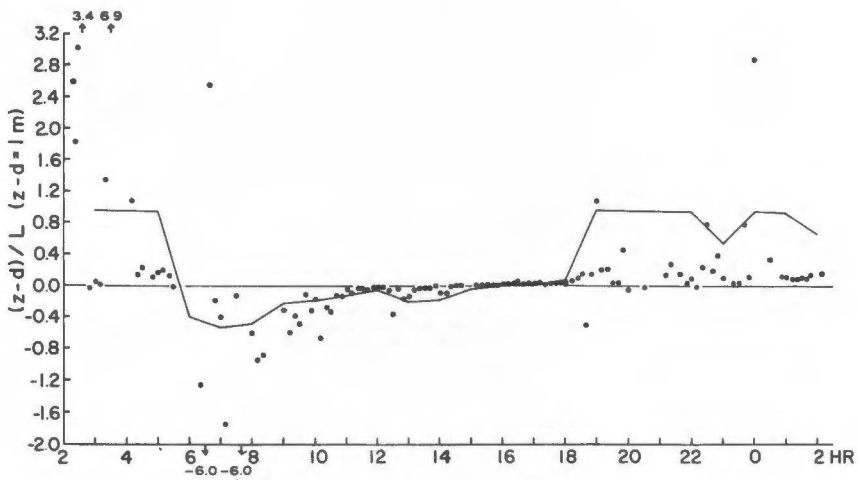

FIG. 7. Time variations of measured Monin-Obukhov stability parameter $(z-d)/L$ with $z-d=1$ m.

The computational inaccuracy inevitable for periods of small fluxes occasionally yields erratically large values in the measured $(z-d)/L$. If this is allowed for, the agreement is fairly good for the daytime; for night the stable stratification is overestimated by the mode.

(6) *Air Temperature* Isopleth representation of temperature given in Fig. 8 shows that the model is able to simulate the daytime warming and nocturnal cooling process in the canopy layer. However, the quantitative agreement is not adequate: the simulated air temperature within canopy is relatively high during the day and relatively low at night compared with observed values. The departure is shown in Fig. 8c. A further significant discrepancy is that with the model the daytime

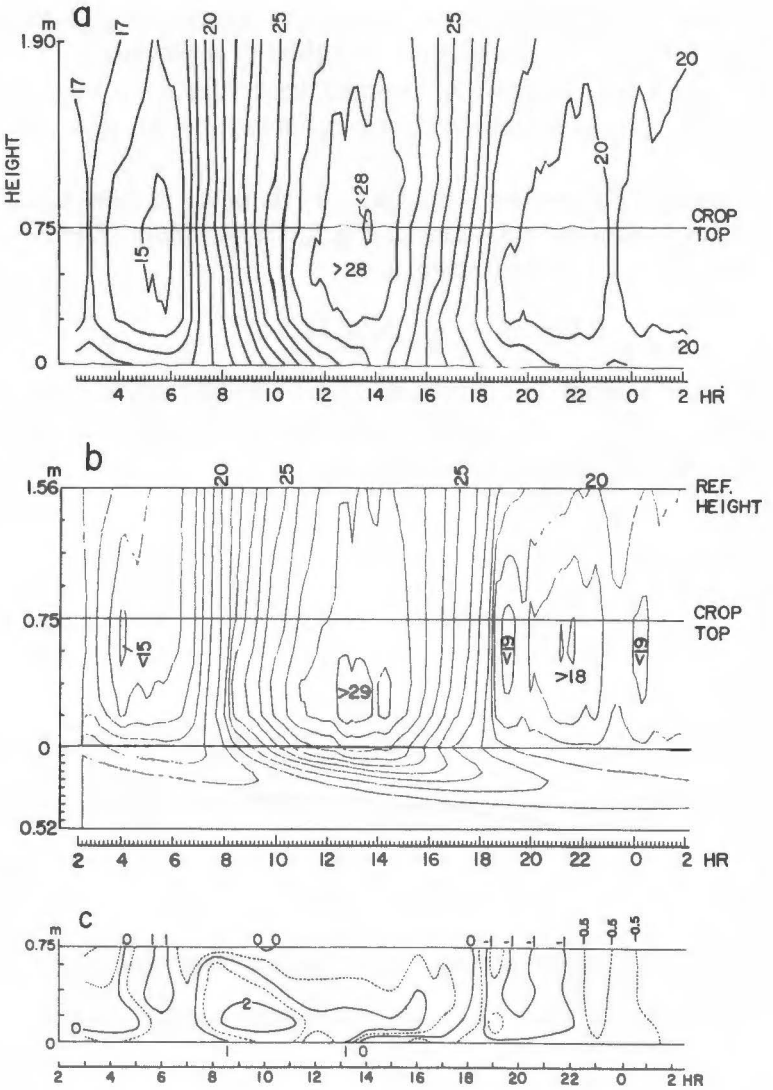

FIG. 8. Isopleth representation of temperature.

(a) Measured air temperature.
(b) Simulated temperature, including soil temperature.
(c) Difference=Simulation-measurement, for air temperature within canopy.

maximum appears in the middle layer of the canopy while in the observation it occurred in the top layer.

The temperature profiles given in Fig. 9 show that model predicts correctly the sense of curvature of the profile. Profiles at 12 h and 24 h are examined in more detail.

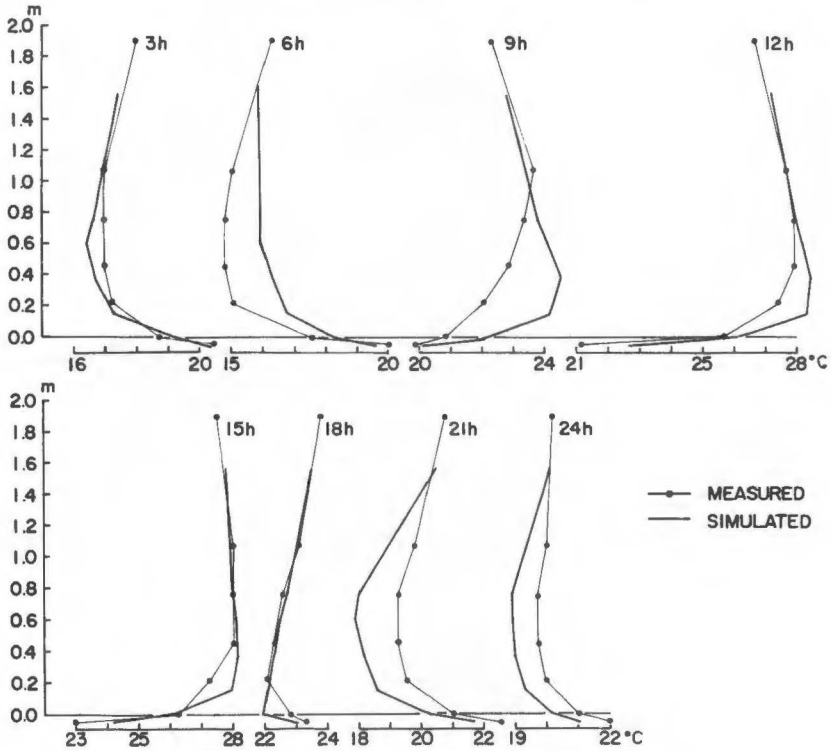

FIG. 9. Measured and simulated temperature profiles.

The profile at 12 h shows that the model simulates well the air temperature at the crop top. Within the canopy the model yields too high temperatures to be explained by the uncertainties ± 0.5°C expected from the sensitivity analysis (Table 1). The stratification is lapse above canopy and stable within canopy. Thus, the difference between model and measurement within canopy suggests that the validity of the ϕ_h function in stable stratification is questionable.

The profile at 24 h shows that the simulated temperatures are about 1°C lower than measurements. The result of the sensitivity analysis (Table 1) shows that the diversion of the outputs is a few tenths of a degree at night. Thus, uncertainties in parameters cannot account for the observed deviation. It is noticed, however, that the forms of profiles within canopy are similar between model and measurement. This implies that most of the deviation can be ascribed to overestimation of the temperature inversion above the canopy. Thus, the validity of the ϕ_h function in stable stratification is again questioned.

The graphs in Fig. 10 shows that the phase of time variation is well simulated by the model.

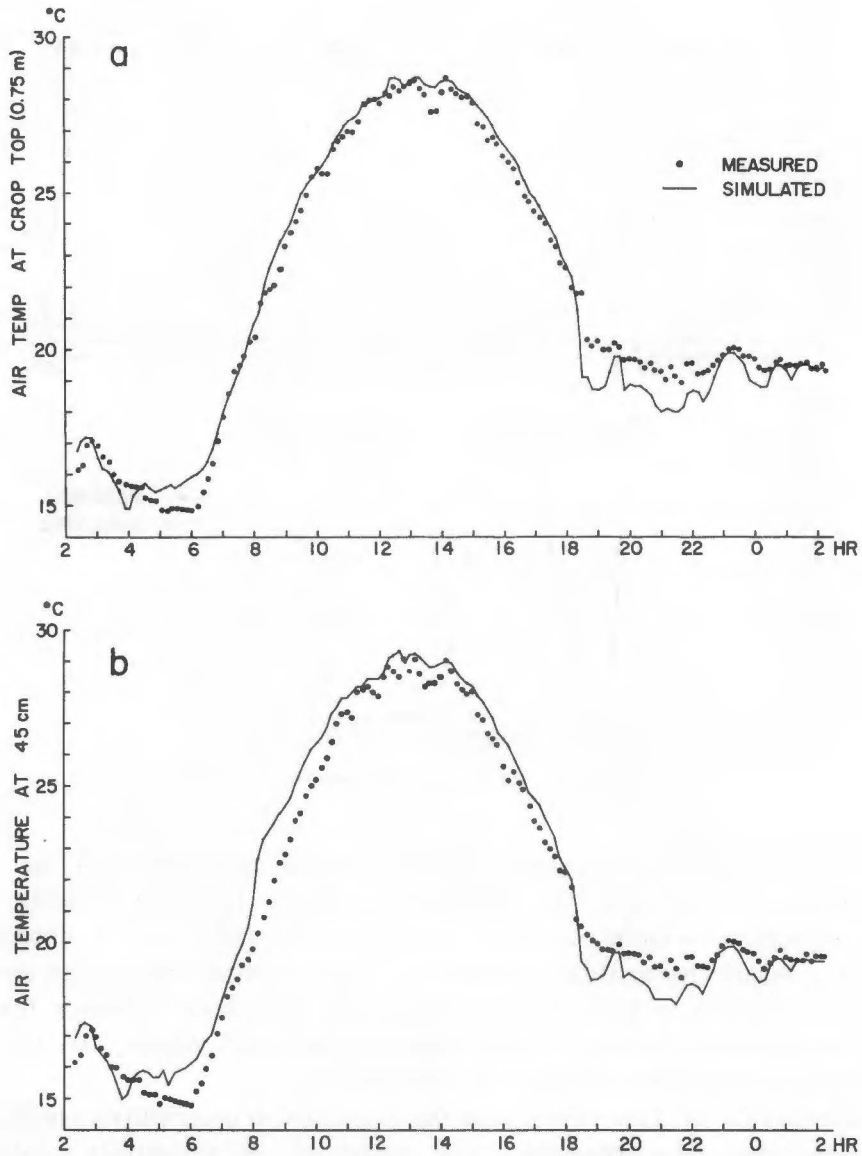

FIG. 10. Measured and simulated time variations of air temperature at the crop top and at 45 cm within canopy; the simulated temperature at 45 cm was interpolated from the values at 27 cm and 60 cm.

(7) *Soil Temperature* Measured and simulated soil temperatures are compared in Fig. 11. Immediately below the ground surface the general trend of variation given by the model is similar to the trend in the experiment. At about 5 cm depth the phase in the model is advanced compared with the observation.

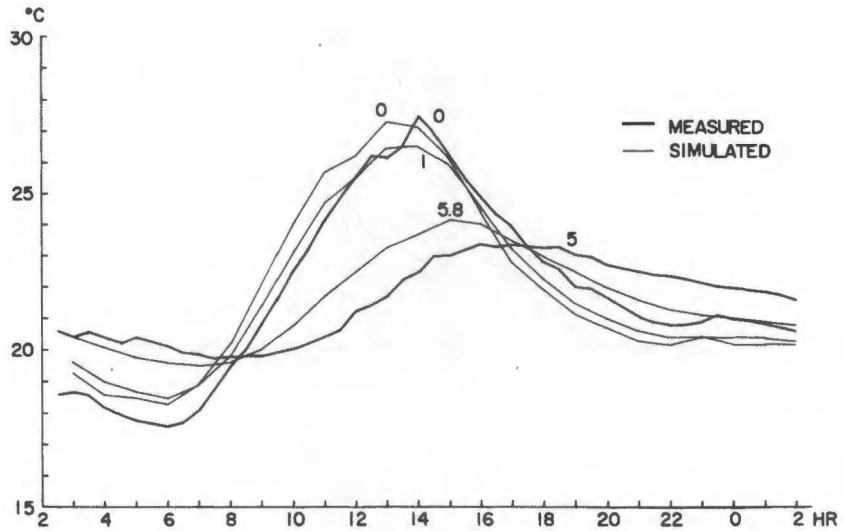

FIG. 11. Time variations of measured and simulated soil temperatures at indicated depth in cm.

Soil temperature was measured at only one location; the measured results may not be representative of the field, and a strict comparison is not feasible.

(8) *Water Vapor* Isopleth representation of vapor pressure (Fig. 12) shows that the model simulates well the daytime buildup of humid region within vegetation. For night, the model predicts formation of a relatively dry region (moisture sink) in the top layer of the canopy. In fact, dew was visible on the leaves of the upper layer of canopy. The observed isopleth indicates that the process is operative, but its effect is not so distinct as in the model.

Fig. 12c shows that the simulated vapor values are lower than the measured vapor pressure except early in the morning.

Profiles of vapor pressure (Fig. 13) show that the model simulates reasonably well the qualitative characteristics of the profile. However, quantitatively the computed results considerably deviate from the measurement, particularly during 6–9 h and at 21 h.

Graphs of Fig. 14 show that the phase of time variation is well simulated by the model.

(9) *Eddy Diffusivity* Fig. 15a compares model values of eddy diffusivity with measured K_q. The latter is given by the procedure described in the section of data processing. The model values are calculated in the evaluation of the flux-gradient relationship. Measured K_q applies for the 190–75 cm layer, while the calculated eddy diffusivity applies for 156–75 cm layer. The calculated variation is similar to the

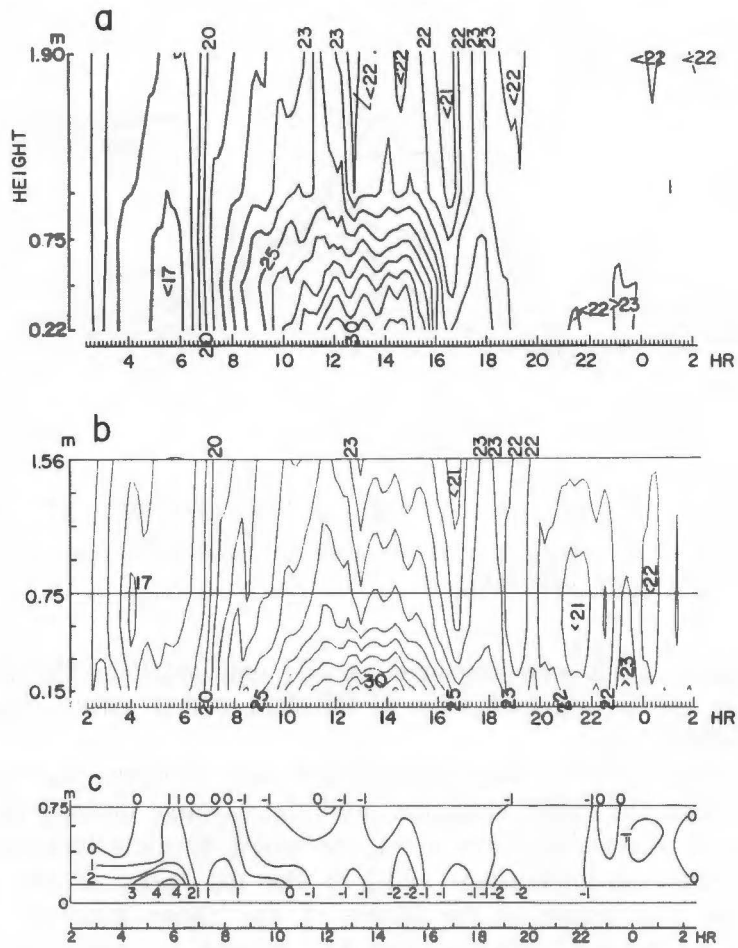

FIG. 12. Isopleth representation of vapor pressure in mb.

(a) Measured vapor pressure.
(b) Simulated vapor pressure.
(c) Difference=simulation–measurement, for vapor pressure within canopy.

observed variation except early in the morning, when the dew evaporation implemented in the model affects the model result.

(10) *CO_2 Flux* CO_2 flux is estimated using K_q determined above and measured ΔC; data on ΔC are given in Fig. 15c shows considerable scatter. The scatter is caused partly by inadequate accuracy in the measurements of ΔC and Δq. In spite of the scatter, the measured diurnal variation is reasonable (see Ohtaki and Seo 1972, 1974).

Fig. 15c shows that the model simulates fairly well the diurnal variation of the CO_2 flux above crop canopy.

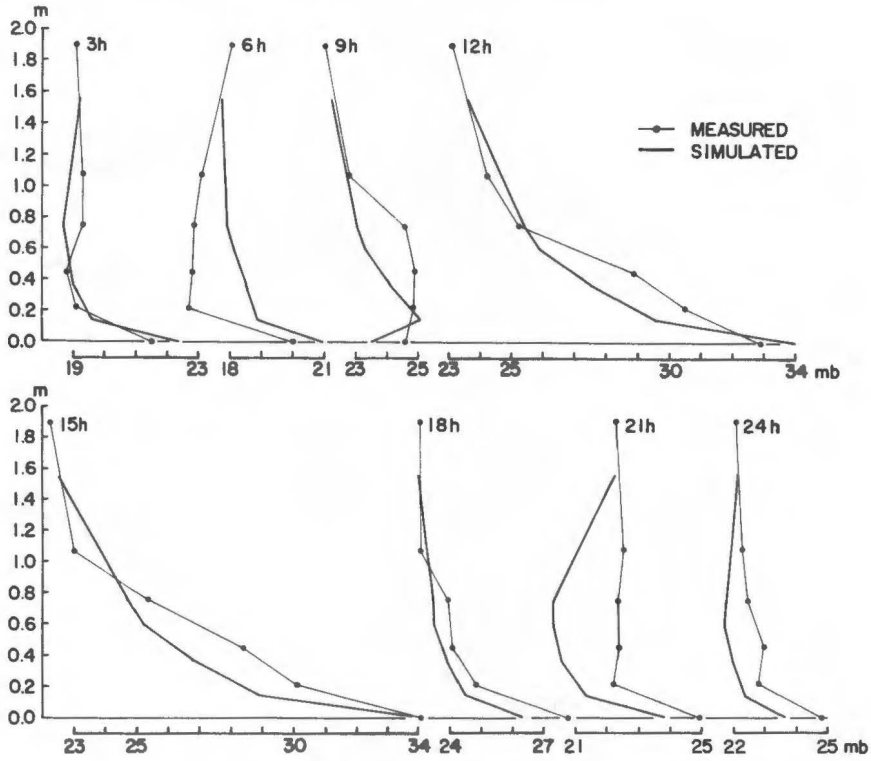

FIG. 13. Measured and simulated profiles of vapor pressure.

The model predicts daytime total of net CO_2 assimilation of 28 g m^{-2}. Soil respiration for the same period amounts to 12 g m^{-2}. The difference 16 g m^{-2} gives CO_2 flux at the crop top. This model value is rather small compared with previous results, 20–30 g m^{-2} in mid-September (Seo and Ohtaki 1974, 1978). The assumed value of soil respiration (1 g m^{-2} h^{-1}) is suspected to be too high.

2. *Some Characteristics of Rice Crop Micrometeorology Predicted by the Model*

We have many outputs that are not amenable to direct comparison with measurement. Some of them are useful to understanding the crop micrometeorology.

(1) *Moisture Budget* Fig. 16 shows the time course of latent heat flux at the crop top and at the soil surface. The soil evaporation amounts to 20% of the evapotranspiration in daily total. It contributes a large fraction to the flux at the crop top in the evening. The sustained evapotranspiration in the evening is a feature characteristic of the rice

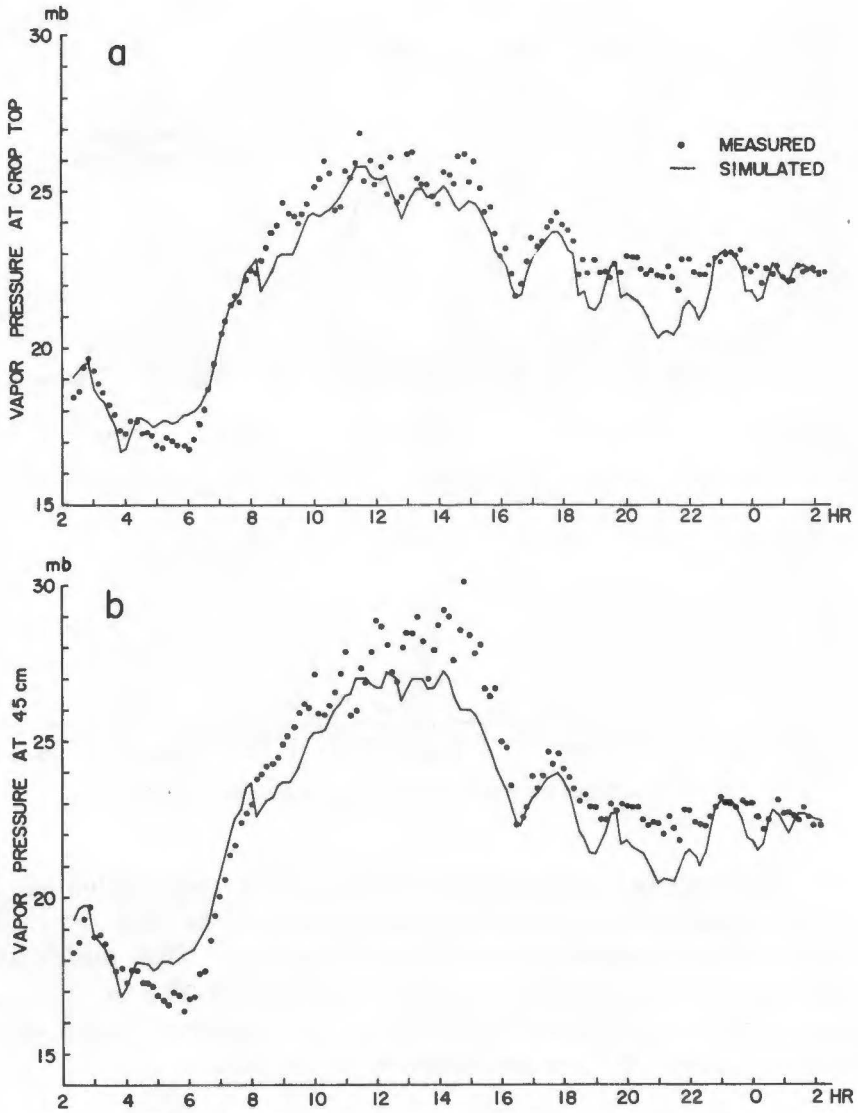

FIG. 14. Measured and simulated time variations of vapor pressure at the crop top and 45 cm within canopy; the simulated vapor pressure at 45 cm was interpolated from the values at 27 cm and 60 cm.

field micrometeorology during the actively growing season (Takeuchi et al. 1980).

Difference of the flux between the top and bottom of the crop layer measures the crop transpiration. When the difference is negative, dew fall is implied. The model predicts dew fall of 0.12 mm over the night. Fig. 16 shows that moisture supplied through soil evaporation plays the major part in the dew deposition on the plant.

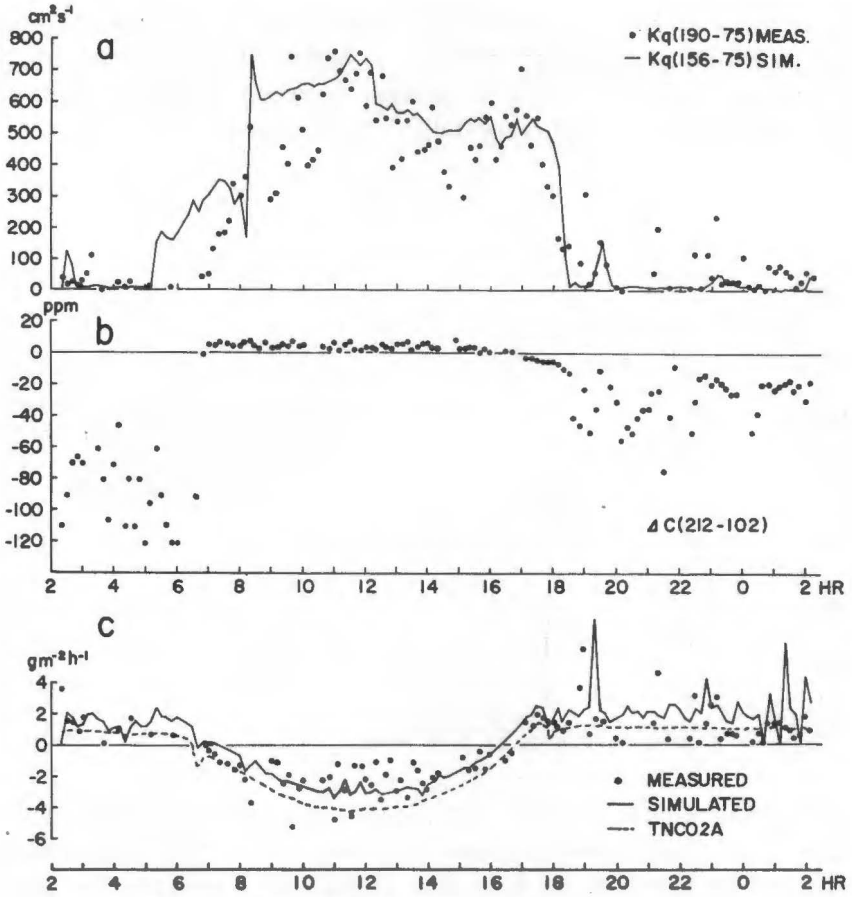

FIG. 15. Time variations of CO_2 flux and the related variables.

(a) Measured and simulated eddy diffusivity for water vapor transfer.
(b) Measured CO_2 difference between 212 cm and 102 cm.
(c) Measured and simulated CO_2 fluxes. Simulated total net CO_2 assimilation (TNCO2A) is included.

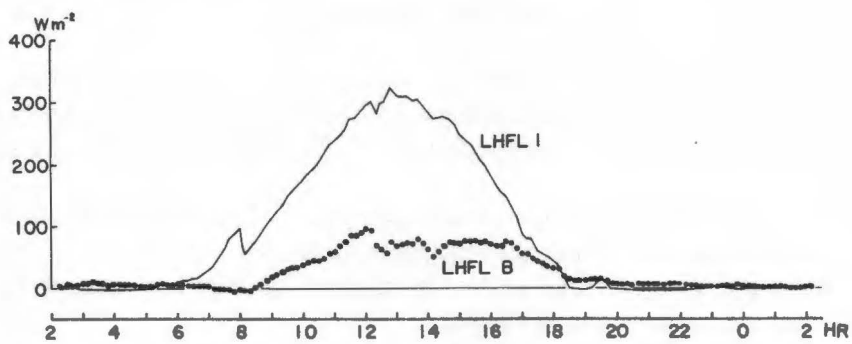

FIG. 16. Simulated latent heat fluxes at the crop top (LHFL1) and at the soil surface (LHFLB).

(2) *Eddy Diffusivity within and above Canopy* Fig. 17 shows the diurnal variation of the eddy diffusivity above the crop and at three heights within the crop. The transition between daytime regime and night regime is very rapid, especially in the evening.

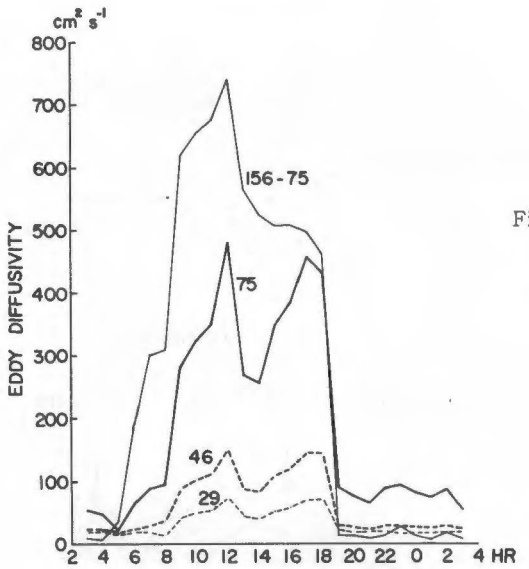

Fig. 17. Simulated eddy diffusivity above canopy (156–75cm), at the crop top (75cm), and two heights within canopy (46, 29cm).

During the night the eddy diffusivity exhibits a maximum at the crop top. This model result is consistent with the vertical distribution of eddy diffusivity obtained by Uchijima (1962). It is remarkable that the above-canopy value is lowest during most of the night period. However, this needs to be reexamined, since the stability correction function is questionable for the stable stratification.

(3) *Distribution of Source and Sink* Fig. 18 shows the diurnal variation of heat and mass exchange between plant and air in the three canopy layers. It is seen that the exchange mainly occurs in the uppermost layer.

Net CO_2 assimilation at night is dark respiration of plant DPL; the present version of the model calculates DPL as function of air temperature above canopy; this gives identical DPL in the three layers having equal LAI.

(4) *Deductions from Sensitivity Analysis* The sensitivity analysis gives the error in the output due to uncertainties in parameters. Table 1 shows that the range of the error is rather limited and cannot affect the preceeding discussions seriously.

Some of the effects of the parameter variation are direct and to be expected; for example, decreased LAI leads to increase in eddy diffusivity

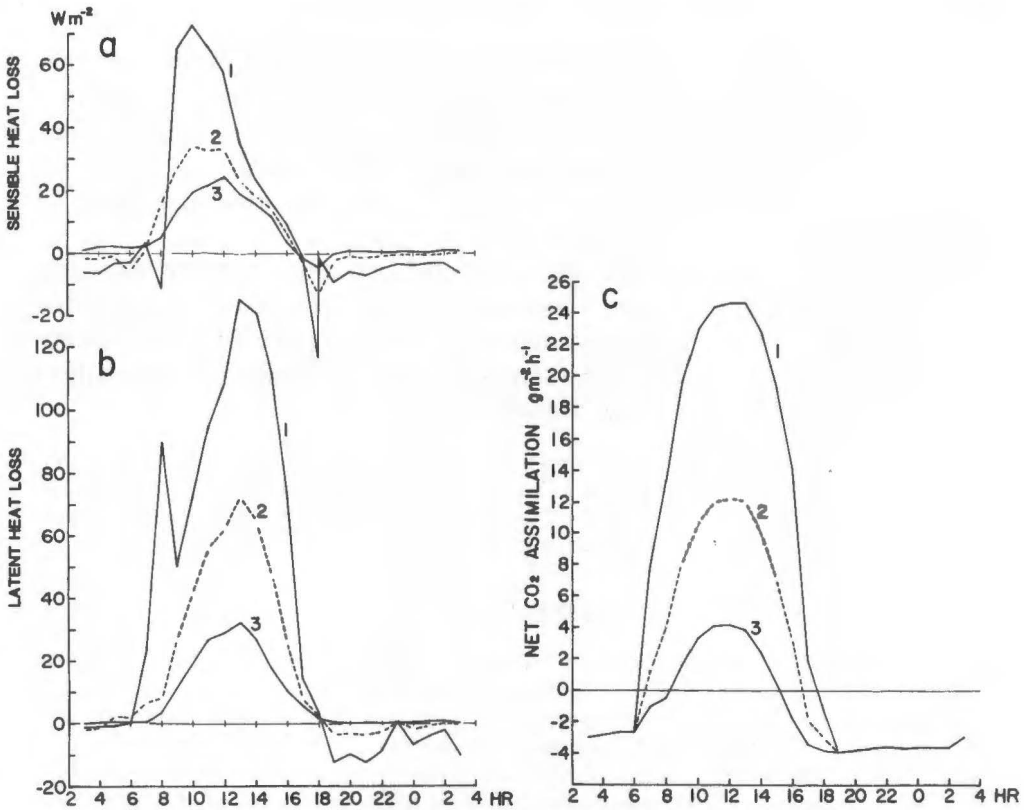

Fig. 18. Simulated distribution of source and sink within canopy ; layer 1 : 75–46 cm, layer 2 : 46–29 cm, layer 3 : 29–0 cm.

(a) Sensible heat loss of canopy,
(b) Latent heat loss of can- opy.
(c) Net CO_2 assimilation.

and decrease of temperature gradient. Others are unexpected and difficult to follow; for example, in daytime an increased RCO2I leads to decrease in leaf resistance and consequent increase in transipiration, and finally results in decrease of temperature gradient.

Some parameters need to be carefully determined to be accurate and representative. These include LAI, DPL, SRESP, and zero-plane displacement.

CONCLUDING REMARKS

The model simulates well the primary characteristics of the rice crop micrometeorology, e. g., large evaporative heat loss of canopy; phase lag of the evaporative flux and phase advance of the sensible heat flux, relative to the phase of net radiation; formation of the thermally active layer within vegetation. It can be concluded that the model is constructed on a physically sound basis.

However, air temperature was predicted too high for the day and too low for the night; water vapor pressure was predicted generally too low. The difference from the measured values is significant. It is likely that most of the deviation arises from the lack of well-established flux-gradient relationship for large stability.

Acknowledgements We would like to express our appreciation to Dr. Y. Miyake for use of the field in the experiment. We are indebted to Dr. K. Kimura and Mr. S. Tanakamaru for measurement of LAI. The senior author (T. Seo) is grateful to Dr. J. Goudriaan for the motivation of this study.

REFERENCES

Carson, D. J. and Richards, P. J. R. 1978. Modelling surface turbulent fluxes in stable conditions. Boundary-Layer Meteorology 14: 67–81.

Goudriaan, J. 1977. Crop Micrometeorology: A Simulation Study. p. 246, Center for Agricultural Publishing and Documentation, Wageningen.

Horie, T. 1978. Studies on photosynthesis and primary production of rice plants in relation to meteorological environments. I. Gaseous diffusive resistances, photosynthesis and transpiration in the leaves as influenced by radiation intensity and wind speed. J. Agr. Met. (Japan) 34: 125–136.

Maitani, T. and Seo, T. 1976. An off-line data acquisition system for micrometeorological observation. Nogaku Kenkyu 55: 215–232. (in Japanese).

Ohtaki, E. and Seo, T. 1972. Measurement of gradient of carbon dioxide and estimation of its flux over a paddy field (1). Ber. Ohara Inst. landw. Biol. Okayama Univ 15: 89–110.

Ohtaki, E. and Seo, T. 1974. Measurement of gradient of carbon dioxide and estimation of its flux over a paddy field (2). Ber. Ohara Inst. landw. Biol. Okayama Univ. 16: 65–77.

Seo, T. 1958. A microclimatological study of thermal exchange at the earth's surface (3). Research Reports of the Kōchi Univ. Vol. 7, No. 21.

Seo, T. 1972. Albedo of several field crops. Ber. Ohara Inst. landw. Biol. Okayama Univ. 15: 111–132.

Seo, T. and Ohtaki, E. 1974. Atmospheric flux of carbon dioxide over paddy fields estimated by heat balance approach. Ber. Ohara Inst. landw. Biol. Okayama Univ. 16: 79–92.

Seo, T. and Ohtaki, E. 1978. Atmospheric flux of carbon dioxide over paddy fields. *In* Ecophysiology of Photosynthetic Productivity. ed. by Monsi, M. and Saeki, T.: 145–151, Univ. of Tokyo Press, Tokyo.

Seo, T. and Yamaguchi, N. 1968. A note on the evapotranspiration from a paddy field. Ber. Ohara Inst. landw. Biol. Okayama Univ. 14: 133–143.

Stigter, C. J., Goudriaan, J., Bottemanne, F. A., Birnie, J., Lengkeek, J. G. and Sibma, L. 1977. Experimental evaluation of a crop climate simulation model for Indian corn

(*Zea mays* L.). Agricultural Meteorology 18: 163–186.

Takasu, K. and Kimura, K. 1972. Microclimate in the field (3): diurnal variations of air temperature, humidity and CO_2 concentration in the rice field. Nogaku Kenkyu 54: 107–120. (in Japanese)

Takeuchi. K., Ohtaki, E. and Seo, T. 1980. Turbulent transfer of water vapor over paddy fields. Ber. Ohara Inst. landw. Biol. Okayama Univ. 18: 1–30.

Uchijima, Z. 1962. Studies on the micro-climate within the plant communities. (1) On the turbulent transfer coefficient within plant layer. J. Agr. Met. (Japan). 18: 1–9.

Uchijima, Z. 1976. Microclimate of the rice crop. *In* Climate and Rice: 115–140, Internat. Rice Res. Inst. Los Banos, Philippines.

Waggoner, P. E. 1975. Micrometeorological Models. *In* vegetation and the Atmosphere. ed. by Monteith J. L. : 205–228, Academic. Press, New York.